Geosci. Model Dev., 8, 2587–2595, 2015
www.geosci-model-dev.net/8/2587/2015/
doi:10.5194/gmd-8-2587-2015

Geoscientific Model Development
Open Access

Photolysis rates in correlated overlapping cloud fields: Cloud-J 7.3c

M. J. Prather

Earth System Science Department, University of California, Irvine, California, USA

Correspondence to: M. J. Prather (mprather@uci.edu)

Received: 29 April 2015 – Published in Geosci. Model Dev. Discuss.: 27 May 2015
Revised: 31 July 2015 – Accepted: 5 August 2015 – Published: 14 August 2015

Abstract. A new approach for modeling photolysis rates (J values) in atmospheres with fractional cloud cover has been developed and is implemented as Cloud-J – a multiple-scattering eight-stream radiative transfer model for solar radiation based on Fast-J. Using observations of the vertical correlation of cloud layers, Cloud-J 7.3c provides a practical and accurate method for modeling atmospheric chemistry. The combination of the new maximum-correlated cloud groups with the integration over all cloud combinations by four quadrature atmospheres produces mean J values in an atmospheric column with root mean square (rms) errors of 4 % or less compared with 10–20 % errors using simpler approximations. Cloud-J is practical for chemistry–climate models, requiring only an average of 2.8 Fast-J calls per atmosphere vs. hundreds of calls with the correlated cloud groups, or 1 call with the simplest cloud approximations. Another improvement in modeling J values, the treatment of volatile organic compounds with pressure-dependent cross sections, is also incorporated into Cloud-J.

1 Introduction

Photolysis, the dissociation of molecules upon absorbing sunlight, drives atmospheric chemistry and controls the composition of the air we breathe. Photolysis rates are governed by the intensity and spectral distribution of sunlight, which is altered by scattering and absorption processes within the atmosphere. Clouds, aerosols, and gases control these processes, but ambiguity in the representation of clouds in atmospheric models is currently the largest source of uncertainty in photolysis rates. This paper presents a new, pragmatic approach for representing the overlap of clouds derived from observations and cloud models, and then provides several practical approximations with marginal computational costs that can be readily incorporated in atmospheric chemistry models. This computer code is a major expansion of Fast-J (Wild et al., 2000; Bian and Prather, 2002; Neu et al., 2007) and is presented here as Cloud-J version 7.3c. Cloud-J contains Fast-J and thus continues that numbering sequence, for which Fast-J 7.2 was the last released version. Fast-J has gone through several variants: Fast-J began with 7 bands, full scattering, for the troposphere; Fast-J2 added 11 bands, absorption only, for the stratosphere; Fast-JX applied full scattering to all 18 bands. Fast-J is used here throughout, although some recent code versions use the JX notation.

Clouds can increase photolysis rates through scattered sunlight, but they can greatly reduce them by shadowing. Modeling the scattering by cloud layers in a column atmosphere and resulting photolysis rates is practical, as in Fast-J, if the layers are horizontally uniform across the modeled air parcel (defined typically as a rectilinear box bounded by latitude, longitude, and pressure surfaces). Clouds layers, however, have horizontal scales of a few kilometers (Slobodda et al., 2015), and thus are represented in global and regional models as fractional coverage in each parcel. In calculating the average photolysis or heating rates through the column atmosphere, one must know how the cloud fractions overlap. Early modeling assumed that model layers consisted of maximally overlapped groups (MAX) that were randomly overlapped relative to one another (MAX-RAN) (Briegleb, 1992; Feng et al., 2004). A more accurate description of cloud overlap is that clouds are highly correlated (i.e., maximally overlapped) when they are vertically near each other, but they become randomly overlapped when separated by greater distances. The cloud decorrelation length is the vertical distance over which the overlap e-folds to random. From a range of observations and cloud models, we estimate a cloud decorrelation length increasing from 1.5 km for the boundary layer to

3 km in the upper troposphere (Pincus et al., 2005; Naud and DelGenio, 2006; Kato et al., 2010; Oreopoulis et al., 2012).

A practical application of this cloud-overlap information, merging maximally overlapped groups that are correlated with each other (MAX-COR), is defined in Sect. 2, where the impact of cloud-overlap models on photolysis rates (J values) is also shown. Cloud-overlap models generate statistics that lead to a large number of weighted independent column atmospheres (ICAs), where the number is too large to be used directly to calculate photolysis or heating rates in global models. Section 3 looks at the simplified cloud models and the approaches to approximate the sum over ICAs, examining their errors. Another recent development in modeling photolysis rates is the treatment of volatile organic compounds with pressure-dependent cross sections, presented in Sect. 4. Recommendations for the cloud-overlap model and the ICA-approximation method are discussed in Sect. 5.

2 Overlap models for fractionally cloudy atmospheres

Typically, meteorological forecasts or climate model data used in atmospheric chemistry models report fractionally cloudy atmospheres (FCAs) in each grid square. Computation of the photolysis or heating rates in an FCA requires knowledge of how the clouds in each layer overlap. The calculation of J values in most atmospheric chemistry models today involves solving the radiative transfer equations in a plane-parallel atmosphere where the vertical layers can be highly inhomogeneous but the horizontal planes are uniform (Stamnes et al., 1988; Wild et al., 2000; Tie et al., 2003). Thus, the only workable method (other than 3-D radiative transfer) is to represent the FCA by a number of ICAs where each ICA is either 100 % cloudy or clear in each layer. The fractional cloud-overlap model determines the layer structure, weighting, and number of ICAs. Other simple cloud models approximate overlap by (i) ignoring clouds entirely (clear sky); (ii) averaging the cloud fraction, f, over each layer, conserving total cloud water (average clouds); and (iii) decreasing the cloud fraction and cloud water in a layer by using a reduced cloud fraction, $f^{3/2}$ followed by averaging across the layer (Briegleb, 1992). These methods are compared with cloud-overlap models in Sect. 3. Here, we focus on how the ICAs differ across cloud-overlap models.

2.1 Random overlap

The ways in which fractionally cloudy layers can overlap is shown schematically in Fig. 1. One assumption is random overlap (RAN). In this case the likelihood (fractional weight, w) of having the cloud in layer L1 fall below the cloud in layer L2 is random and hence equals f^{L1}. This particular pairing – cloud below cloud – becomes ICA #1. Superscripts in the equations below refer to atmospheric layers. The likelihood for the clear layer under the cloudy layer is by default

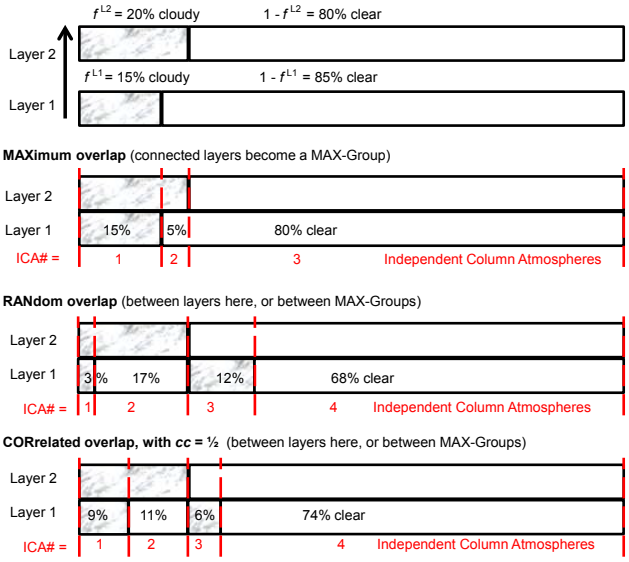

Figure 1. Schematic of overlapping fractional cloud layers. See text.

the complement.

$$w^{\mathrm{L1}}(\#1) = f^{\mathrm{L1}} \tag{1}$$

$$w^{\mathrm{L1}}(\#2) = 1 - f^{\mathrm{L1}} \tag{2}$$

The likelihood of the cloudy layer in L2 above is

$$w^{\mathrm{L2}}(\#1) = w^{\mathrm{L2}}(\#2) = f^{\mathrm{L2}}. \tag{3}$$

The total weight W for each ICA #1 and #2 is then the product of w^{L1} and w^{L2}.

$$\begin{aligned} W^{\mathrm{L1\text{-}L2}}(\#1) &= w^{\mathrm{L1}}(\#1)w^{\mathrm{L2}}(\#1) = f^{\mathrm{L1}}f^{\mathrm{L2}} \\ &= 0.15 \times 0.20 = 3\,\% \text{ (see Fig. 1)} \end{aligned} \tag{4}$$

$$\begin{aligned} W^{\mathrm{L1\text{-}L2}}(\#2) &= w^{\mathrm{L1}}(\#2)w^{\mathrm{L2}}(\#2) = (1 - f^{\mathrm{L1}})f^{\mathrm{L2}} \\ &= 0.85 \times 0.20 = 17\,\% \end{aligned} \tag{5}$$

Similar rules apply to ICAs #3 and #4,

$$w^{\mathrm{L1}}(\#3) = f^{\mathrm{L1}} \text{ and } w^{\mathrm{L2}}(\#3) = 1 - f^{\mathrm{L2}}, \tag{6}$$

$$w^{\mathrm{L1}}(\#4) = 1 - f^{\mathrm{L1}} \text{ and } w^{\mathrm{L2}}(\#4) = 1 - f^{\mathrm{L2}}, \tag{7}$$

and thus

$$\begin{aligned} W^{\mathrm{L1\text{-}L2}}(\#3) &= w^{\mathrm{L1}}(\#3)w^{\mathrm{L2}}(\#3) = f^{\mathrm{L1}}(1 - f^{\mathrm{L2}}) \\ &= 0.15 \times 0.80 = 12\,\% \text{ (see Fig. 1)}, \end{aligned} \tag{8}$$

$$\begin{aligned} W^{\mathrm{L1\text{-}L2}}(\#4) &= w^{\mathrm{L1}}(\#4)w^{\mathrm{L2}}(\#4) = (1 - f^{\mathrm{L1}})(1 - f^{\mathrm{L2}}) \\ &= 0.85 \times 0.80 = 68\,\%. \end{aligned} \tag{9}$$

ICAs #1 and #3 are tagged as cloudy in L1, and ICAs #2 and #4 are tagged as clear in L1. The sum of cloudy fractions in L1 must be conserved: $3\,\% + 12\,\% = 15\,\% = f^{\mathrm{L1}}$. One of the problems in implementing a full-RAN model is that the number of ICAs scales as 2^{NL}, where NL is the number of cloudy layers in the RAN group.

2.2 Correlated overlap

When correlated, the likelihood of a cloudy layer lying under a cloud above is greater than random, $w^{\mathrm{L1}}(\#1) > f^{\mathrm{L1}}$, by a factor of $g^{\mathrm{L1}} > 1$. The cloud correlation factor cc ranges from 0 (random) to 1 (maximal overlap), and g^{L1} is the interpolating function linear in cc between random and maximal overlap.

$$g^{\mathrm{L1}} = 1 + \mathrm{cc}(1/f^{\mathrm{L2}} - 1),$$
$$\text{subject to } g^{\mathrm{L1}} \le 1/f^{\mathrm{L1}} \text{ and } g^{\mathrm{L1}} \le 1/f^{\mathrm{L2}} \quad (10)$$

Hence for cc > 0 we have an increased likelihood of the cloud in L1 falling underneath the cloud in L2. For the example in Fig. 1, cc = 0.5 and $g^{\mathrm{L1}} = 3$.

$$w^{\mathrm{L1}}(\#1) = g^{\mathrm{L1}} f^{\mathrm{L1}} = 3 \times 0.15 = 45\,\% \quad (11)$$

$$w^{\mathrm{L1}}(\#2) = 1 - g^{\mathrm{L1}} f^{\mathrm{L1}} = 1 - 0.45 = 55\,\% \quad (12)$$

The likelihood of clouds in L1 falling below the clear section in L2 is reduced and is calculated from the requirement that the sum of cloudy fractions in L1 is still f^{L1}.

$$w^{\mathrm{L1}}(\#3) = f^{\mathrm{L1}}(1 - g^{\mathrm{L1}} f^{\mathrm{L2}})/(1 - f^{\mathrm{L2}}) = 0.15 \times (1 - 3 \times 0.20)/0.80 = 7.5\,\% \quad (13)$$

By complement, the weighting of clear sky in layer L1 under clear sky in layer L2 is

$$w^{\mathrm{L1}}(\#4) = 1 - w^{\mathrm{L1}}(\#3) = 1 - 0.075 = 92.5\,\%. \quad (14)$$

Note that if cc = 0, or $f^{\mathrm{L2}} = 1$, or $f^{\mathrm{L1}} = 1$, then $g^{\mathrm{L1}} = 1$ and correlated overlap (COR) defaults to RAN. The two additional limits on g^{L1} in Eq. (10) are required to keep $w^{\mathrm{L1}}(\#2)$ and $w^{\mathrm{L1}}(\#3)$ positive. The w^{L2} weights do not include a g factor.

$$w^{\mathrm{L2}}(\#1) = w^{\mathrm{L2}}(\#2) = f^{\mathrm{L2}} \quad (15)$$

$$w^{\mathrm{L2}}(\#3) = w^{\mathrm{L2}}(\#4) = (1 - f^{\mathrm{L2}}) \quad (16)$$

The combined ICA weights are

$$W^{\mathrm{L1\text{-}L2}}(\#1) = w^{\mathrm{L1}}(\#1) w^{\mathrm{L2}}(\#1) = g^{\mathrm{L1}} f^{\mathrm{L1}} f^{\mathrm{L2}} = 3 \times 0.15 \times 0.20 = 9\,\%, \quad (17)$$

$$W^{\mathrm{L1\text{-}L2}}(\#2) = w^{\mathrm{L1}}(\#2) w^{\mathrm{L2}}(\#2) = (1 - g^{\mathrm{L1}} f^{\mathrm{L1}}) f^{\mathrm{L2}} = 0.55 \times 0.20 = 11\,\%, \quad (18)$$

$$W^{\mathrm{L1\text{-}L2}}(\#3) = w^{\mathrm{L1}}(\#3) w^{\mathrm{L2}}(\#3) = f^{\mathrm{L1}}(1 - g^{\mathrm{L1}} f^{\mathrm{L2}}) = 0.15 \times 0.40 = 6\,\%, \quad (19)$$

$$W^{\mathrm{L1\text{-}L2}}(\#4) = w^{L1}(\#4) w^{\mathrm{L2}}(\#4) = 1 - f^{\mathrm{L2}} - f^{\mathrm{L1}} + g^{\mathrm{L1}} f^{\mathrm{L1}} f^{\mathrm{L2}} = 1 - 0.20 - 0.06 = 74\,\%. \quad (20)$$

As in RAN, ICAs #1 and #3 are tagged as cloudy in layer L1, ICAs #2 and #4 are tagged as clear in layer L1, and the sum of cloudy fractions is conserved ($9\,\% + 6\,\% = 15\,\% = f^{\mathrm{L1}}$) but with different weightings. The COR model also has ICAs scaling as 2^{NL}.

2.3 Maximal overlap

For maximal overlap of clouds (MAX) as in Fig. 1, the two layers L1 and L2 form a MAX group G1 consisting of one clear-sky column (80 % fractional coverage) and 2 cloudy columns – one with clouds in both layers ($f_1^{\mathrm{G1}} = 15\,\%$) and one with a cloud only in the upper layer L2 ($f_2^{\mathrm{G1}} = 5\,\%$). For a MAX group, there can be several ICAs with cloud fractions, each with a unique combination of cloudy layers. The clear-sky column does not occur if any of the MAX layers has a cloud fraction of 100 %. For continuous cloud fractions, the number of ICAs equals the number of unique cloud fractions present (plus 1 if clear sky is present).

A MAX group is characterized by the number of cloudy columns (N1) consisting of combinations of cloudy or clear sky in different layers of the group and having a fractional area equal to f_1^{G1}, f_2^{G1}, f_3^{G1}, $\ldots f_{\mathrm{N1}}^{\mathrm{G1}}$. The total cloudy fraction is $F^{\mathrm{G1}} = f_1^{\mathrm{G1}} + f_2^{\mathrm{G1}} + f_3^{\mathrm{G1}} + \ldots + f_{\mathrm{N1}}^{\mathrm{G1}} \le 1$, with the (possible) clear-sky column fraction of $1 - F^{\mathrm{G1}}$, giving N1 + 1 ICAs for that group. As in the earlier Fast-J work (Neu et al., 2007), the cloud fractions in Cloud-J are quantized to limit the number of ICAs in a MAX group. The examples here use 10 bins, and hence cloud fractions are limited to 0, 10, 20, 30, … 100 %. With this binning, the in-cloud water content is scaled to conserve the cloud-water content in each layer. This approximation is now resolution independent in terms of the number of model layers and limits each MAX group to 10 ICAs.

2.4 Maximal groups with correlated overlap

The MAX-COR model generates ICAs from upper and lower layers that are MAX groups. For a general approach, we assume that the upper group G2 consists of N2 cloudy column members with fractions $f_1^{\mathrm{G2}} + f_2^{\mathrm{G2}} + f_3^{\mathrm{G2}} + \ldots + f_{\mathrm{N2}}^{\mathrm{G2}} = F^{\mathrm{G2}}$ and one clear-sky column member of fraction $1 - F^{\mathrm{G2}}$. Similarly, the lower group G1 has N1 + 1 ICAs (see Sect. 2.3). Each of the N1 + 1 ICAs in group G1 are paired with the N2 + 1 ICAs above in group G2. The total number of ICAs combining both groups is the product (N1 + 1)(N2 + 1), assuming that there are clear-sky members in both groups. The ICA sequence defining each unique pairing (J1, J2) is then

$$(1,1),(2,1),(3,1),\ldots(\mathrm{N1}+1,1),(1,2),(2,2),(3,2),\ldots(\mathrm{N1}+1,\mathrm{N2}+1), \quad (21)$$

such that ICA #M is composed of members

$$\mathrm{J1} = (\mathrm{M}-1) \text{ modulo } (\mathrm{N1}+1) + 1, \quad (22)$$

$$\mathrm{J2} = \text{integer } ((\mathrm{M}-1)/(\mathrm{N1}+1)) \text{ modulo } (\mathrm{N2}+1) + 1. \quad (23)$$

The cloud correlation factor of group G1 with group G2 is the same for all cloudy ICAs and is derived from the total

cloudy fractions F^{G1} and F^{G2}.

$$g^{G1} = 1 + \mathrm{cc}(1/F^{L2} - 1),$$
$$\text{subject to } g^{G1} \le 1/F^{G1} \text{ and } g^{G1} \le 1/F^{G2} \quad (24)$$

For convenience denote J1 ≤ N1 as cloudy^{G1}, J1 = N1 + 1 as clear^{G1}, J2 ≤ N2 as cloudy^{G2}, and J2 = N2 + 1 as clear^{G2}. Then the weightings for the G1 members are

$$w^{G1}\ (\text{cloudy}^{G1},\ \text{cloudy}^{G2}) = g^{G1} f_{J1}^{G1}, \quad (25)$$
$$w^{G1}\ (\text{clear}^{G1},\ \text{cloudy}^{G2}) = 1 - g^{G1}\left(f_1^{G1} + f_2^{G1} + f_3^{G1} + \ldots + f_{N1}^{G1}\right) = 1 - g^{G1} F^{G1}. \quad (26)$$

By conserving each cloudy group member's fractional area in G1, the weights under G2 clear sky are

$$w^{G1}\ (\text{cloudy}^{G1},\ \text{clear}^{G2}) = f_{J1}^{G1}(1 - g^{G1} F^{G2})/(1 - F^{G2}), \quad (27)$$
$$w^{G1}\ (\text{clear}^{G1},\ \text{clear}^{G2}) = 1 - F^{G1}(1 - g^{G1} F^{G2})/(1 - F^{G2}). \quad (28)$$

All of these formulae also work if $F^{G1} > F^{G2}$ and if $F^{G1} = 0$ or 1 (same for F^{G2}). A special case of MAX-COR is MAX-RAN when cc = 0. With the cloud fractions binned into 10 intervals, then the number of ICAs for MAX-COR or MAX-RAN models scales as 10^{NG}, where NG is the number of MAX groups.

2.5 *J* value errors

Our recommended cloud-overlap model uses the information on vertical correlations (Pincus et al., 2005; Naud and DelGenio, 2006; Kato et al., 2010; Oreopoulis et al., 2012), which shows cloud decorrelation lengths on the order of 1.5 km in the lower atmosphere increasing to 3 km or more in the upper troposphere. Since a true COR model scales as 2^{NL} and becomes rapidly impractical for high-resolution models, we define vertical groups of cloud layers globally according to the decorrelation lengths: 0–1.5 km altitude, 1.5–3.5, 3.5–6, 6–9, 9–13, and > 13 km. We assume that the cloud layers within a decorrelation length are highly correlated with one another and thus form a MAX group. When such MAX groups are adjacent they have a mean separation of one decorrelation length, and we choose a cloud correlation factor of cc = 0.33, similar to 1 *e*-fold. When there is a clear-sky gap between a pair of G6 layers, the MAX groups are separated by more than one decorrelation length; thus, we reduce the factor cc with successive multiples (i.e., with two missing G6 MAX groups between two cloudy layers, the effective cc = $0.33^3 = 0.036$). This model is denoted G6/.33. Two other G6 models were tested: cc = 0.00 corresponds to randomly overlapped adjacent groups (MAX-RAN, G6/.00); and cc = 0.99 is almost maximally overlapped (MAX, G6/.99).

In looking at how this model aligned the clouds for realistic FCAs, we found that extensive cirrus fractions in the uppermost layers prevented the expected overlap of small-fraction cumulus below. Thus, a seventh MAX group is added if there was a cirrus shield (defined from top down as adjacent ice-only clouds with $f > 0.5$). Because of the cloud-fraction binning into 10 % intervals, the number of ICAs is bounded by 5×10^6 (including the cirrus shield). This limit is resolution independent and was never reached in any FCAs examined here (highest number of ICAs for one FCA was 3500). The major computational cost comes with the Fast-J computation, and the methods for approximating the average of *J* values over all ICAs (Sect. 3) use at most four Fast-J calculations no matter how many ICAs.

Two other cloud-overlap models tested here are the MAX-RAN groupings G0 and G3 (Feng et al., 2004; Neu et al., 2007). Model G0 assumes that all vertically adjacent cloudy layers are a MAX group (maximally overlapped), and all such groups separated by a clear layer are RAN overlapped. This model seems logical but has difficulty finding a clear layer when the FCA has been averaged over several hours or taken from a parameterized cloud-resolving model. It our tests, using meteorological data with NL = 36, the maximum number of G0 ICAs was 375. Model G3 has at most three MAX-RAN groups demarcated by atmospheric regimes: a fixed altitude (1.5 km, stratus top) and temperature (the liquid-to-ice cloud transition). The maximum possible number of ICAs per FCA for G3 is 10^3, and in our tests we found 288.

Our recommended cloud-overlap model is G6/.33 since it is based on the observed–modeled cloud decorrelation lengths. For a given FCA, we treat the *J* values calculated by summing Fast-J over all the ICAs generated by G6/.33 as the correct value. We calculate errors for the other cloud-overlap models (here) or various ICA-approximation models using the G6/.33 model (Sect. 3). The errors in photolysis rates are calculated for different cloud-overlap models by generating all the ICAs, using Fast-J to calculate *J* values, and computing the weighted sum of *J*'s. This study focuses on two *J* values that are critical in tropospheric chemistry and emphasize different wavelength ranges from near 300 nm, where O_3 absorption and molecular scattering are important, to 600 nm, where clouds are the predominant factor. J-O^1D refers to the photolysis rate of $O_3 + h\nu \rightarrow O_2 + O(^1D)$; and J-NO_3 includes both channels of the rate of $NO_3 + h\nu \rightarrow NO + O_2$ and $NO_2 + O$. We tested other key *J* values like those of HNO_3 and NO_2, but found that their errors fell between the first two.

The *J* value tests are summarized in Table 1. We use a high-resolution snapshot from the European Center for Medium-range Weather Forecasts, similar to what is used (at lower resolution) in the UC Irvine and University of Oslo chemistry-transport models (Søvde et al., 2012; Hsu and Prather, 2014). The 640 FCAs are a 3 h average of a single longitudinal belt just above the Equator (T319L60 Cycle 36)

Table 1. Models for cloud overlap and approximation of ICAs including errors in J values.

Cloud-overlap models to generate ICAs		ICAs[a]	avg err 0–1 km		rms error 0–1 km		rms error 0–16 km	
			J-O^1D	J-NO_3	J-O^1D	J-NO_3	J-O^1D	J-NO_3
G0	MAX-RAN with MAX groups bounded by layers with CF = 0	19	+2 %	+2 %	21 %	17 %	6 %	11 %
G3	3 MAX-RAN groups split at 1 km and at the ice-only cloud level	21	+2 %	+2 %	15 %	15 %	5 %	7 %
G6/.00	6 MAX-COR groups, cc = 0.00	169	−1 %	−1 %	5 %	4 %	2 %	3 %
G6/.33	6 MAX-COR groups, cc = 0.33[b]	169						
G6/.99	6 MAX-COR groups, cc = 0.99	169	+2 %	+1 %	11 %	8 %	4 %	7 %
	Simple cloud models	ICAs						
ClSky	clear sky, ignore clouds	1	+14 %	+10 %	24 %	20 %	14 %	23 %
AvCld	average fractional cloud across layer	1	−5 %	+1 %	11 %	11 %	8 %	15 %
CF3/2	increase CF to $CF^{3/2}$ and average over layer	1	+7 %	+11 %	10 %	15 %	5 %	8 %
	ICA approximations	J calls						
AvDir	average direct beam from all ICAs	1	+5 %	+11 %	6 %	13 %	3 %	7 %
MdQCA	quadrature column atmospheres uses mid-point in each QCA	2.8	+1 %	0 %	4 %	4 %	4 %	5 %
AvQCA	QCAs, uses average in each QCA[b]	2.8	−1 %	0 %	3 %	2 %	2 %	4 %
Ran-3	Select 3 ICAs at random	3	+2 %	+1 %	12 %	12 %	9 %	12 %

[a] Average number of ICAs for a tropical atmosphere; see Fig. 2. [b] Recommended cloud-overlap model and reference model for calculation of errors.

and have clouds only in the lowermost 36 layers. Profiles of temperature and ozone are taken from tropical mean observations; the Rayleigh-scattering optical depth at 600 nm is about 0.12, and a mix of aerosol layers has a total optical depth of 0.23. J value errors are calculated separately for each FCA and then averaged. The number of ICAs per FCA averages 169 for model G6, 21 for model G3, and 19 for model G0; see Fig. 2 for the probability distribution of ICA numbers. Errors are pressure weighted and include the average error over 0–1 km altitude, the root mean square (rms) error over 0–1 km, and the full tropospheric rms error (0–16 km). The average 0–1 km differences across the models are small (< 2 %), but the rms 0–1 and 0–16 km differences are large, indicating that 640 different FCAs produce canceling errors in the mean. The rms errors for G0 and G3 are worrisome: more than 15 % in the boundary layer and 5 to 11 % in the full troposphere. The G6 errors are almost linear with the cc value. The G6/.99 with highly correlated overlap is similar to G3 which has MAX overlap throughout most of the atmosphere. The G6/.00 with random overlap is the closest to the correlated model G6/0.33.

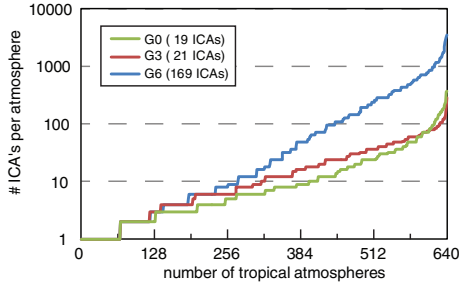

Figure 2. Number of independent column atmospheres (ICAs) generated by three different cloud-overlap models (G0, G3, G6) from 640 different tropical fractionally cloudy atmospheres (FCAs) and sorted in order of increasing ICA number. The different cloud correlation factors used in the G6 model do not change the number of ICAs, only their weights. The average number of ICAs per FCA is given in the legend. See text for definition of models.

3 Approximating the exact sum over ICAs

Quadrature column atmospheres (QCAs) have been defined previously (Neu et al., 2007) as four representative ICA-like atmospheres that represent four domains of ICAs with total cloud optical depths at 600 nm of 0–0.5 (clear sky), 0.5–4 (cirrus-like), 4–30 (stratus-like), and > 30 (cumulus-like). The original model sorted the ICA optical depths to get the weightings of each QCA and then picked the ICA that occurred at the mid-point in terms of fractional area (MdQCA). Thus, there can be up to four separate calls to Fast-J for each of the QCAs, but on average there are 2.8 QCAs per FCA be-

cause not all four of the QCA ranges of cloud optical depths (0–0.5, 0.5–5, 5–30, > 30) are present in each FCA. Here we extend that approach with three new methods for approximating the integral over ICAs: define each QCA from the average ICAs in its domain (AvQCA); use the averaged direct solar beam from all ICAs to derive an effective scattering optical depth from clouds in each layer (AvDir); and selecting three random ICAs based on their weights (Ran-3; with comparable computational costs to either QCA).

The AvQCA model comes easily from the MdQCA formalism, but all ICAs in each of the four total optical depth domains are used to calculate the average cloud-water content in each QCA. The AvDir model calculates the weighted direct solar beam from each ICA, where only 600 nm cloud extinction is included. In this case it was found that an equivalent isotropic extinction is needed as in two-stream methods (Joseph et al., 1976), and we scaled the optical depth of each cloud layer by a factor of $1-1.1P_1/3$, with a minimum value of 0.04. P_1 (3 times the asymmetry factor) is the second term in the Legendre expansion of the scattering phase function for the cloud in that layer. The derived optical depth in each layer is calculated from the reduction in direct beam across the layer (Beer–Lambert law) and put into the single Fast-J calculation with the original cloud properties of that layer, not the equivalent isotropic properties.

In addition to these ICA approximations, we also compare the G6/.33 exact sum over ICAs with three simple cloud models often used in chemistry models that do not generate ICAs: clear sky (ClSky); averaged cloud over each layer (AvCld); and cloud fraction to the $3/2(f^{3/2}$, CF3/2).

A sample of mean and rms errors for the seven approximate methods is given in Table 1. In addition, a tropospheric profile of the mean bias in J values is shown in Fig. 3. As expected the ClSky and AvCld methods show opposite biases and large rms errors. The CF3/2 method produces reasonable averages, but still has rms errors of 10 % or more. The AvDir method does not perform as well as expected and looks only slightly better than CF3/2; however, the profile of mean error (Fig. 3) is preferable to that of CF3/2. Both QCA methods performed excellently and deliver rms errors of less than 5 % with mean biases in the boundary layer on the order of ±1 %. The new AvQCA method has smaller rms errors, but the original MdQCA method has a slightly better profile for the mean error. Ran-3 is computationally comparable to the QCAs; it has a reasonable mean bias as expected given the number of samples (3×640), but a much worse rms error, typically > 10 %.

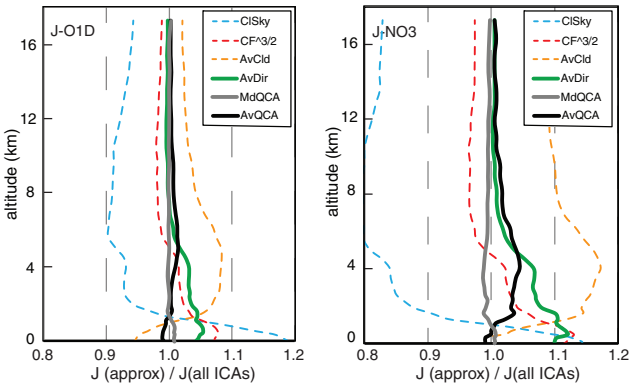

Figure 3. Profile of the average bias in J value approximations relative to the J value calculated from the weighted average of all ICAs using model G6/.33. Values here are calculated using a solar zenith angle of 13.6° and a surface albedo of 0.10 and averaged over 640 FCAs (108, 125 ICAs) derived from the equatorial statistics (all longitudes) of cloud fraction, liquid water content, and ice water content from a snapshot of a T319L60 meteorology from the European Centre for Medium-range Weather Forecasts. Three simple cloud methods (dashed lines) do not use any cloud-overlap model, and three approximations for the ICAs (solid lines) use the G6/.33 model described here. The MdQCA ICA approximation was developed in Neu et al. (2007); the AvQCA and AvDir approximations are developed in this paper. The J-O^1D refers to the photolysis rate of $O_3 + h\nu \rightarrow O_2 + O(^1D)$, with average values of 4 ($z = 0$ km) to 9 ($z = 16$ km) $\times\, 10^{-5}\ s^{-1}$; and J-NO_3, to all channels of the rate $NO_3 + h\nu \rightarrow$, with average values of 2 to $4 \times 10^{-1}\ s^{-1}$. These two J values emphasize sunlight from 310 to 600 nm, and thus span the typical range of errors in tropospheric photolysis rates.

4 Cloud-J and volatile organic compounds

Volatile organic compounds (VOCs) cover a wide class of gaseous species containing C, H, O and sometimes N or S. They play a major role in the chemical reactivity of the troposphere, including production and loss of O_3 and loss of CH_4 (e.g., Jacob et al., 1993; Horowitz et al., 1998; Ito et al., 2009; Emmons et al., 2010), plus the formation of secondary organic aerosols (SOAs; e.g., Ito et al., 2007; Fu et al., 2008; Galloway et al., 2011). For most VOCs (and H_2O_2) photolysis is the dominant loss; see Fig. 4. Daily photolysis rates (loss frequencies) range from 0.03 to 20 per day and some vary greatly with altitude. For 9 of the 14 species shown in Fig. 4, the photolysis rates are larger or comparable to the loss rates for reaction with OH (given in the legend). Thus, accurate calculation of their J values is important in atmospheric chemistry models.

VOCs present a particular problem for any photolysis code that averages over wavelength intervals. For most chemical species, cross sections including quantum yields are parameterized as a function of wavelength (ν) and temperature (T) (e.g., Atkinson et al., 2008; Sander et al., 2011). In this case, Fast-J calculates solar-flux-weighted, average cross sections for each wavelength bin (Wild et al., 2000; Bian and Prather, 2002). These tables are created for a set of fixed T's, and then the cross section used for each bin in each atmospheric layer is interpolated in T. Many VOCs have complex, pressure-dependent quantum yields (e.g., Blitz et al., 2006) that follow the Stern–Volmer formulation, where

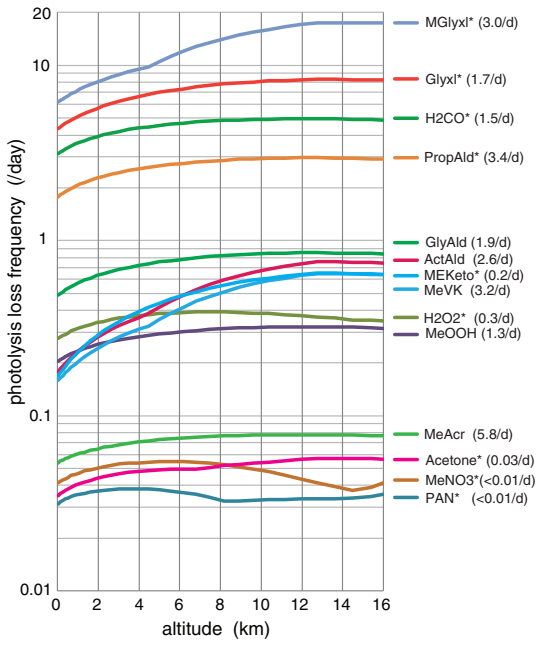

Figure 4. Volatile organic compounds (VOCs) and related species photolysis rates (per day) as a function of altitude (km). The complex structure with altitude is due to a combination of increasing UV radiation with altitude and Stern–Volmer pressure dependences on quantum yields. Changes in slope occur at the interpolation points, temperature, or pressure of the cross sections. We assume that the 12:00 LT J's (clear-sky, tropical atmosphere, albedo = 0.10, SZA = 15°) apply for 8 of 24 h. Equivalent rates for OH loss are shown with the species name in the legend and assume a 12:00 LT OH density of 6×10^6 cm^{-3}. Asterisks denote species for which photolysis loss is greater than or comparable to OH loss. VOC abbreviations are MGlyxl: methyl glyoxal, Glyxl: glyoxal, PropAld: propionaldehyde, GlyAld: glycol aldehyde, ActAld: acetaldehyde, MEKeto: methylethyl ketone, MeVK: methylvinyl ketone, MeOOH: CH_3OOH, MeAcr: methacrolein, MeNO3: methyl nitrate, and PAN: peroxyacetyl nitrate.

photolysis cross sections (for dissociation) are a function of wavelength, temperature, and pressure (P), typically of the form $A(T, \upsilon)/(1 + B(T, \upsilon)P)$, where A and B can be rational polynomial functions of T and υ (see Sander et al., 2011). For most VOCs the pressure dependence changes across the wavelengths within a model bin, and thus the T dependence averaged cross sections has different values at different P, but cannot be simply post-interpolated as a function of P because of the wavelength dependence of B. A 2-D set of cross sections for each wavelength bin, interpolated as a function of T and P, could be developed but would add to the complexity and cost of Fast-J.

Recognizing that VOCs are predominantly tropospheric and that T and P are highly correlated in the troposphere, Cloud-J, and the new Fast-J that sits within it, has devised an alternative method of interpolating the cross sections for each atmospheric layer: T is the traditional method used for most species; but P is used for VOCs with highly pressure-dependent quantum yields. For P interpolation, the cross sections are averaged over wavelength at three points along a typical tropospheric lapse rate: 0 km, 295 K, 999 hPa; 5 km, 272 K, 566 hPa; and 13 km, 220 K, 177 hPa. Currently species with P interpolation include: acetaldehyde, methylvinyl ketone, methylethyl ketone, glyoxal, methyl glyoxal, and one branch of acetone photolysis. Fast-J does not extrapolate beyond its supplied tables, and thus currently it applies 177 hPa cross sections for these VOCs throughout the stratosphere, but this has minimal impact on stratospheric chemistry. Depending on the available laboratory data, the number of cross section tables per species in the new Fast-J (either T or P interpolation) can be 1, 2, or 3. Cloud-J, new with version 7.3, includes an updated version of Fast-J version 7.1, whose only change is in the formatting of the input files to allow for more flexible numbering and labeling of species with their cross sections and of the cloud–aerosol scattering tables.

5 Discussion and recommendations

We recommend use of the G6/.33 MAX-COR model for cloud overlap with AvQCA to approximate the average photolysis rates over the ICAs. This combination of algorithms best matches the exact solution for average J values at a single time within each FCA. Averaging J values for an air parcel that includes a mix of cloudy and clear air is not the same as averaging the chemical reactivity across cloudy and clear. Nevertheless, for species with photolysis rates that are less than the frequency at which clouds form and air is processed through them (on the order of 24 day^{-1}), the average J is the relevant quantity for chemistry modeling.

A next step would be to model at high-enough resolution so that air parcels are either cloudy or clear. This could resolve the 3-D correlation of clouds at scales of 1–4 km, which will in turn require a 3-D radiative transfer model (Norris et al., 2008; Davis and Marshak, 2010). A more interesting approach that is practical with typical global model resolution is the treatment of inhomogeneous cloud fields as being composed of independently scattering cloudlets (Petty, 2002). This cloudlet approximation could be readily integrated into the plane-parallel framework of Fast-J.

The added computational cost with G6/.33+AvQCA occurs with the additional calls to Fast-J, as the MAX-COR model and sorting of ICAs is fast. Computing photolysis rates 2.8 times per atmospheric column instead of once may add to the overall computational burden, but Fast-J is efficient and the costs will be much less than the overall chemistry-solver and tracer-transport codes.

Code availability

The most recent version of Cloud-J and earlier versions of Fast-J can be found at ftp://128.200.14.8/public/prather/Fast-J/. Cloud-J 7.3c as described here is included as a zip file and includes new coding to correct failures in compilation or execution (v7.3b) as well as reducing the cloud correlation factor when there are decorrelation-length gaps between any of the MAX-COR groups (v7.3c). Although with v7.3c some J values changed in the third decimal place, changes in the GMDD figures and tables were undiscernible. Subscribe to the listserv UCI-Fast-J@uci.edu or check the ftp site for updates. Send questions or suggestions for Cloud-J features to the listserv or the author (mprather@uci.edu).

The Supplement related to this article is available online at doi:10.5194/gmd-8-2587-2015-supplement.

Acknowledgements. Research at UCI was supported by NASA grant NNX13AL12G and DOE BER award DE-SC0012536. The author is indebted to T. Reddmann, R. Sander and an anonymous reviewer for finding the coding inconsistencies/errors, and Cloud-J should now be more reliable across platforms.

Edited by: R. Sander

References

Atkinson, R., Baulch, D. L., Cox, R. A., Crowley, J. N., Hampson, R. F., Hynes, R. G., Jenkin, M. E., Rossi, M. J., Troe, J., and Wallington, T. J.: Evaluated kinetic and photochemical data for atmospheric chemistry: Volume IV – gas phase reactions of organic halogen species, Atmos. Chem. Phys., 8, 4141–4496, doi:10.5194/acp-8-4141-2008, 2008.

Bian, H. S. and Prather, M. J.: Fast-J2: accurate simulation of stratospheric photolysis in global chemical models, J. Atmos. Chem., 41, 281–296, 2002.

Blitz, M. A., Heard, D. E., and Pilling, M. J.: Study of acetone photodissociation over the wavelength range 248–330 nm: evidence of a mechanism involving both the singlet and triplet excited states, J. Phys. Chem. A, 110, 6742–6756, doi:10.1021/Jp056276g, 2006.

Briegleb, B. P.: Delta-Eddington Approximation for solar-radiation in the NCAR Community Climate Model, J. Geophys. Res., 97, 7603–7612, 1992.

Davis, A. B. and Marshak, A.: Solar radiation transport in the cloudy atmosphere: a 3-D perspective on observations and climate impacts, Rep. Prog. Phys., 73, 026801, doi:10.1088/0034-4885/73/2/026801, 2010.

Emmons, L. K., Apel, E. C., Lamarque, J.-F., Hess, P. G., Avery, M., Blake, D., Brune, W., Campos, T., Crawford, J., DeCarlo, P. F., Hall, S., Heikes, B., Holloway, J., Jimenez, J. L., Knapp, D. J., Kok, G., Mena-Carrasco, M., Olson, J., O'Sullivan, D., Sachse, G., Walega, J., Weibring, P., Weinheimer, A., and Wiedinmyer, C.: Impact of Mexico City emissions on regional air quality from MOZART-4 simulations, Atmos. Chem. Phys., 10, 6195–6212, doi:10.5194/acp-10-6195-2010, 2010.

Feng, Y., Penner, J. E., Sillman, S., and Liu, X.: Effects of cloud overlap in photochemical models, J. Geophys. Res., 109, D04310, doi:10.1029/2003JD004040, 2004.

Fu, T. M., Jacob, D. J., Wittrock, F., Burrows, J. P., Vrekoussis, M., and Henze, D. K.: Global budgets of atmospheric glyoxal and methylglyoxal, and implications for formation of secondaryorganic aerosols, J. Geophys. Res., 113, D15303, doi:10.1029/2007JD009505, 2008.

Galloway, M. M., Loza, C. L., Chhabra, P. S., Chan, A. W. H., Yee, L. D., Seinfeld, J. H., and Keutsch, F. N.: Analysis of photochemical and dark glyoxal uptake: implications for SOA formation, Geophys. Res. Lett., 38, L17811, doi:10.1029/2011GL048514, 2011.

Horowitz, L. W., Liang, J. Y., Gardner, G. M., and Jacob, D. J.: Export of reactive nitrogen from North America during summertime: sensitivity to hydrocarbon chemistry, J. Geophys. Res., 103, 13451–13476, 1998.

Hsu, J. N. and Prather, M. J.: Is the residual vertical velocity a good proxy for stratosphere–troposphere exchange of ozone?, Geophys. Res. Lett., 41, 9024–9032, doi:10.1002/2014gl061994, 2014.

Ito, A., Sillman, S., and Penner, J. E.: Eects of additional nonmethane volatile organic compounds, organic nitrates, and direct emissions of oxygenated organic species on global tropospheric chemistry, J. Geophys. Res., 112, D06309, doi:10.1029/2005JD006556, 2007.

Ito, A., Sillman, S., and Penner, J. E.: Global chemical transport model study of ozone response to changes in chemical kinetics and biogenic volatile organic compounds emissions due to increasing temperatures: sensitivities to isoprene nitrate chemistry and grid resolution, J. Geophys. Res., 114, D09301, doi:10.1029/2008jd011254, 2009.

Jacob, D. J., Logan, J. A., Yevich, R. M., Gardner, G. M., Spivakovsky, C. M., Wofsy, S. C., Munger, J. W., Sillman, S., Prather, M. J., Rodgers, M. O., Westberg, H., and Zimmerman, P. R.: Simulation of summertime ozone over North-America, J. Geophys. Res., 98, 14797–14816, 1993.

Joseph, J. H., Wiscombe, W. J., and Weinman, J. A.: Delta-Eddington Approximation for radiative flux-transfer, J. Atmos. Sci., 33, 2452–2459, 1976.

Kato, S., Sun-Mack, S., Miller, W. F., Rose, F. G., Chen, Y., Minnis, P., and Wielicki, B. A.: Relationships among cloud occurrence frequency, overlap, and effective thickness derived from CALIPSO and CloudSat merged cloud vertical profiles, J. Geophys. Res., 115, D00H28, doi:10.1029/2009JD012277, 2010.

Naud, C. and DelGenio, A. D.: Cloud Overlap Dependence on Atmospheric Dynamics, Sixteenth ARM Science Team Meeting Proceedings, 27–31 March 2006, Albuquerque, NM, 2006.

Neu, J. L., Prather, M. J., and Penner, J. E.: Global atmospheric chemistry: integrating over fractional cloud cover, J. Geophys. Res., 112, D11306, doi:10.1029/2006JD008007, 2007.

Norris, P. M., Oreopoulos, L., Hou, A. Y., Taod, W.-K., and Zenga, X.: Representation of 3-D heterogeneous cloud fields using copulas: theory for water clouds, Q. J. Roy. Meteor. Soc., 134, 1843–1864, 2008.

Oreopoulos, L., Lee, D., Sud, Y. C., and Suarez, M. J.: Radiative impacts of cloud heterogeneity and overlap in an atmospheric General Circulation Model, Atmos. Chem. Phys., 12, 9097–9111, doi:10.5194/acp-12-9097-2012, 2012.

Petty, G. W.: Area-average solar radiative transfer in three-dimensionally inhomogeneous clouds: the Independently Scattering Cloudlet Model, J. Atmos. Sci., 59, 2910–2929, 2002.

Pincus, R., Hannay, C., Klein, S. A., Xu, K.-M., and Hemler, R.: Overlap assumptions for assumed probability distribution function cloud schemes in large-scale models, J. Geophys. Res., 110, D15S09, doi:10.1029/2004JD005100, 2005.

Sander, S. P., Friedl, R. R., Abbatt, J. P. D., Barker, J. R., Burkholder, J. B., Golden, D. M., Kolb, C. E., Kurylo, M. J., Moortgat, G. K., Wine, P. H., Huie, R. E., and Orkin, V. L.: Chemical Kinetics and Photochemical Data for Use in Atmospheric Studies, Evaluation No. 17, Jet Propulsion Laboratory, Pasadena, CA, 2011.

Slobodda, J., Hünerbein, A., Lindstrot, R., Preusker, R., Ebell, K., and Fischer, J.: Multichannel analysis of correlation length of SEVIRI images around ground-based cloud observatories to determine their representativeness, Atmos. Meas. Tech., 8, 567–578, doi:10.5194/amt-8-567-2015, 2015.

Søvde, O. A., Prather, M. J., Isaksen, I. S. A., Berntsen, T. K., Stordal, F., Zhu, X., Holmes, C. D., and Hsu, J.: The chemical transport model Oslo CTM3, Geosci. Model Dev., 5, 1441–1469, doi:10.5194/gmd-5-1441-2012, 2012.

Stamnes, K., Tsay, S. C., Wiscombe, W., and Jayaweera, K.: Numerically stable algorithm for discrete-ordinate-method radiative-transfer in multiple-scattering and emitting layered media, Appl. Optics, 27, 2502–2509, 1988.

Tie, X. X., Madronich, S., Walters, S., Zhang, R. Y., Rasch, P., and Collins, W.: Effect of clouds on photolysis and oxidants in the troposphere, J. Geophys. Res., 108, 4642, doi:10.1029/2003jd003659, 2003.

Wild, O., Zhu, X., and Prather, M. J.: Fast-J: accurate simulation of in- and below-cloud photolysis in tropospheric chemical models, J. Atmos. Chem., 37, 245–282, 2000.